Progress In Electromagnetics Research M, Vol. 96, 99–107, 2020

A Highly Bendable Log-Periodic Array Antenna for Flexible Electronics

Hattan Abutarboush[1, *], Omar Siddiqui[1], Muhammad Wali[2], and Farooq Tahir[2]

Abstract—An eleven element log-periodic dipole-array (LPDA) antenna, occupying a surface area of only $90 \times 52\,\text{mm}^2$, printed on an ultra-thin flexible Kapton substrate of thickness 0.035 mm, is proposed. The antenna operates with a stricter 10 dB reflection coefficient bound in the frequency bands 2.75–3.53 GHz and 4–6.2 GHz. For a less stringent bound of 6 dB (which is acceptable for wearable applications), it operates in the wider range of 2.7–6.8 GHz. The antenna has an end-fire radiation pattern with a maximum measured gain of 6 dBi. The flexibility of the antenna is illustrated by reflection and radiation pattern measurements for three different radii, i.e., 50, 30, and 10 mm in both the convex and concave configurations. It is experimentally demonstrated that LPDA exhibits stable input-impedance characteristics and consistent radiation properties over the whole operating band under all bending conditions. The low cost, light weight, and flexible design, as well as the broadband performance in both concave and convex bent configurations, prove the suitability of the antenna for the contemporary flexible electronic devices.

1. INTRODUCTION

Recently, a renewed interest has been demonstrated in flexible, highly-directive planar antennas [1–10]. With low profile and conformal configurations, these flexible antennas find numerous applications in emerging technologies such as sensor networks, internet of things (IoT), and wearable electronics [11]. To acquire highly flexible antenna designs, unconventional substrates such as kapton [2–4], paper [7], and plastics [9] have been explored. In addition to flexibility, the antennas for wireless communications should also demonstrate stable radiation properties and gain throughout the operational spectrum [7]. Hence antenna analysis over all the bending conditions is an integral part of the design and measurement procedure [1, 5].

The design principle of log-periodic antenna is based on emphasizing the angle of its final geometrical shape leading to frequency-independent impedance and radiation properties [12, 13]. Out of many possible logarithmic variants, the log-periodic dipole array (LPDA) has become popular, probably because of its design and implementation simplicity. Wire-based or printed forms of LPDAs have been traditionally applied in broadband applications, such as shortwave radio [14, 15]. Lately, LPDAs have also been effectively employed in nonconventional applications, such as wireless sensor networks, which need a larger bandwidth or use multiple operational bands [16–18]. For sensor networks, in particular, the use of ultrawide band (UWB) offers significant benefits over narrowband because of its inherent robustness against the hostile environment of interference and fading [16]. With the additional bendable designs, the antennas can be applied in communication applications where flexibility feature is highly desired, such as in foliage and agriculture sensing [19]. There are challenges for designing and implementing the antenna on very thin substrates. In particular, achieving large bandwidth is a

Received 14 July 2020, Accepted 31 August 2020, Scheduled 12 September 2020
* Corresponding author: Hattan Abutarboush (habutarboush@taibahu.edu.sa).
[1] College of Engineering, Taibah University, Madinah, Saudi Arabia. [2] Research Institute for Microwave and Millimeter-wave Studies (RIMMS), National University of Sciences and Technology, Islamabad, Pakistan.

difficult task since the bandwidth of resonant antennas is known to vary inversely with the substrate's thickness [20]. Moreover, a comprehensive flexibility analysis is useful for researchers working in this area. The proposed LPDA antenna can also cover many applications in the sub-7 GHz bands such as WLAN and 5G [1, 21, 22].

Several research studies in recent past focussed on the design of LPDAs with stable broadband electromagnetic properties [6, 8, 9, 23–27]. The antennas were printed either on rigid substrates such as Arlon, Rogers, FR4 or on 1 mm thick PET substrates and hence cannot be considered for highly flexible electronics. The LPDA presented in [7], on the other hand, demonstrated limited flexibility due to a relatively thicker paper substrate (of 0.5 mm thickness) and also because of the coaxial feed that limited the bending features.

In this paper, we investigate the electromagnetic characteristics of a broadband LPDA antenna designed on an ultra-thin Kapton film substrate having a thickness of 0.035 mm. The motivation came from studying some of the broadband LPDA designs [25–29] in which compactness was achieved by deforming the basic dipole structure. For example, the LPDAs of [25, 28] were based on Koch-shaped dipoles, while [29] and [27] employed meandered and sinusoidally varying dipoles geometries, respectively. Some of the recently designed high gain antenna arrays are compared with the proposed LPDA in Table 1. In the given designs, we notice rather stable radiation properties, in spite of the geometrical deformation of the constituting dipoles. Therefore, with the proposed Kapton-based LPDA, we anticipate consistent impedance properties and radiation patterns under the specified bending configurations. Moreover, by applying a rugged CPW feed, the antenna is designed to be more flexible than its paper predecessor [7]. We further provide a comprehensive bending analysis of the antenna in which broadband antenna parameters are measured over a wide range of bending radii. Such a thorough flexibility analysis, according to our opinion, has not been presented in the contemporary LPDA literature. We chose Kapton as it was readily available during the design and fabrication of the antenna. For commercial designs, other more thermally stable and moisture-resistant substrates such as cellulose nanopaper can be considered [30].

Table 1. Comparison of proposed antenna with other flexible and non-flexible Yagi Uda, Quasi Yagi and LPDAs antennas.

Ref.	Size	Gain (dBi)	Flexibility	Application
[4]	Not Given	8	Not Flexible	ISM Band (24.5 GHz)
[5]	0.0731λ	5.76	Limited Flexibility (RT Duroid 0.127 mm Substrate)	On Chip and Medical
[6]	0.3496λ	8.8	Not Flexible	Ultra-wide band
[7]	0.8308λ	9.5	Limited Flexibility (Photo-paper 0.5 mm Substrate)	Ultra-wide band
[8]	$0.3504\ \lambda$	5.2	Not Flexible	GPS, UWB, X-band
[9]	0.396λ	5.5	Not Flexible	Bluetooth and WLAN
[23]	0.468λ	6.85	Not Flexible	Broadband
[24]	0.1548λ	4	Not Flexible	EMC Measurement
[25]	0.105λ	5	Not Flexible	RFID Readers
[26]	0.651λ	8.5	Not Flexible	Conformal load-bearing antennas
[27]	0.1064λ	5.5	Not Flexible	High Power Airborne
Proposed	0.384λ	8	Highly Flexible (Kapton 0.035 mm Substrate)	Wideband and Multi-band

2. ANTENNA DESIGN

The LPDA is designed by standard procedure laid out by Carrel [31] and followed by [9, 23, 27]. The two characteristic parameters, i.e., the bandwidth and directivity of an LPDA are determined by its

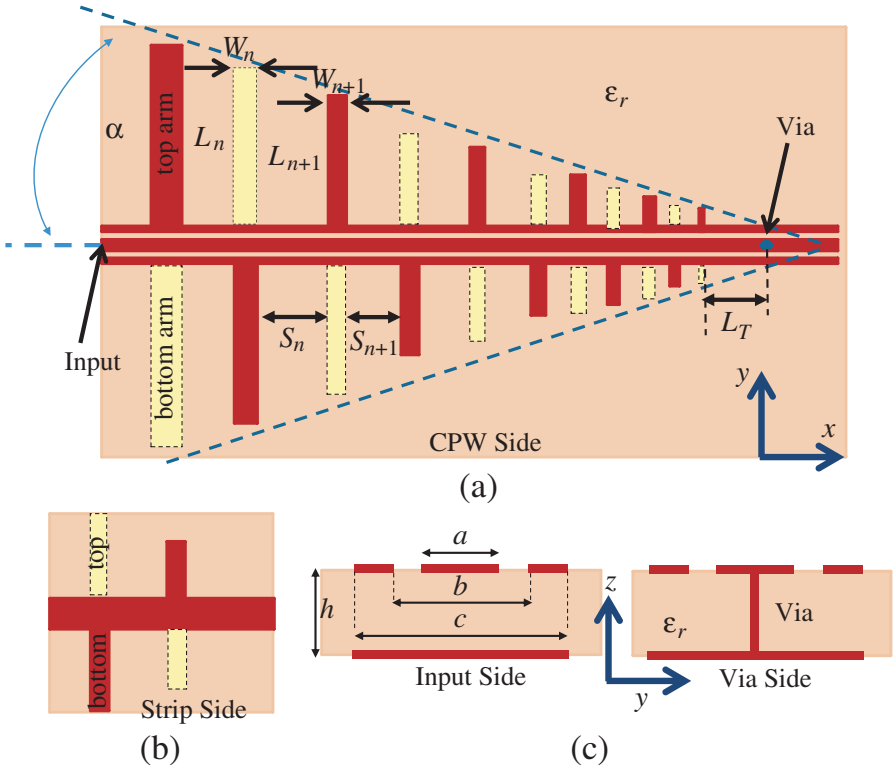

Figure 1. (a) The top view of the proposed Kapton-based 11-element LPDA antenna. The dipole elements are fed by a finite-ground CPW on the top side and a single strip on bottom side. The total surface area ($x \times y$) is $90 \times 52\,\text{mm}^2$. The distance between via and last element (L_T) is 6.8 mm. The rest of the dimensions are given in Table 1. (b) The bottom view of only a smal part of the LPDA showing the strip fed dipole arms. (c) Lateral view of the substrate cross-section. The input side, showing the dimensions of the CPW and the parallel strip, where $a = 1.1\,\text{mm}$, $b = 1.7\,\text{mm}$, and $c = 2\,\text{mm}$). The via side shows how the central conductor of CPW is connected to the strip.

spacing factor $\sigma = S_n/4L_n$ and the scaling factor $\tau = L_{n+1}/L_n$ [31] (see the geometry in Fig. 1 for the parameter definitions). From the design curves given in [31, 32], the geometric parameters τ and σ for 7 dB directivity LPDA are given by 0.875 and 0.12, respectively. The aperture angle α and active region bandwidth B_{AR} can then be calculated by,

$$\alpha = \tan^{-1}\left(\frac{1-\tau}{4\sigma}\right), \quad B_{AR} = 1.1 + 7.7(1-\tau)^2 \cot\alpha \tag{1}$$

For the given input parameters, the values of aperture angle and active region bandwidth are given by 14.6° and 1.56, respectively. The operating bandwidth B is the ratio of the spectral edges, which is approximated by 3 if the two frequencies are given by 2.5 and 6.8 (i.e., $f_{\max}/f_{\min} = 3$). Once τ, B, and B_{AR} are determined, the number of elements (N) of the LPDA antenna is calculated by using [31, 32]:

$$N = 1 + \frac{\ln(B \cdot B_{AR})}{\ln\left(\frac{1}{\tau}\right)} \tag{2}$$

By putting all the required parameters in above equations, the value of N comes out to be 12.55, which is rounded down to 11, considering the compactness of the structure. Next step in the design procedure is the determination of the actual dipole sizes of the printed LPDA version. The half-wave dipole representing the lowest LPDA operational frequency ($f_{\min}$) is first optimized on the Kapton polyimide-based substrate using the full-wave HFSS simulator. Targeting a good impedance match and wider bandwidth, the length (L_1) and width (W_1) of the largest dipole are given by 23.5 mm and

Table 2. The dimensions of the dipole elements of the LPDA antenna.

Dipole	L_n (mm)	W_n (mm)	S_n (mm)
1	23.5	3.87	-
2	20.56	3.53	9.74
3	17.32	3.23	9
4	12.43	2.96	8.785
5	10.5	2.72	8.34
6	8.24	2.52	7.69
7	7.13	2.33	4.89
8	6.15	2.17	4.527
9	5.3	2.03	4.16
10	4.54	1.91	2.98
11	3.87	1.5	3.36

3.87 mm, respectively. The dimensions of the rest of the LPDA elements are then calculated by the well-known logarithmic rule:

$$\tau = \frac{L_{n+1}}{L_n} = \frac{W_{n+1}}{W_n} = \frac{Sn+1}{S_n} \tag{3}$$

The complete design of Fig. 1 layout is summarized in Table 2. As depicted in Fig. 1(a), the top layer contains a finite-ground CPW that feeds one of the arms of each dipole. A portion of the bottom layer is depicted in Fig. 1(b), which comprises a strip parallel to the CPW feeding the second arms of the dipoles. The antenna is fabricated by the additive manufacturing process in which highly conductive copper is deposited to form radiators on both sides of the substrate. Both sides of the fabricated antenna prototype along with a demonstration of its flexibility are depicted in Fig. 2. The 11 element array forms a compact broadband antenna occupying a surface area of only $90 \times 52\,\text{mm}^2$.

For impedance consistency, the CPW feed is designed to match with the $50\,\Omega$ input connector. The CPW parameters a, b, and c (as shown in Fig. 1(c)) are computed using the well-known CPW design equations [33] and optimized using CST tool. The antenna is fed from the input side through an SMA

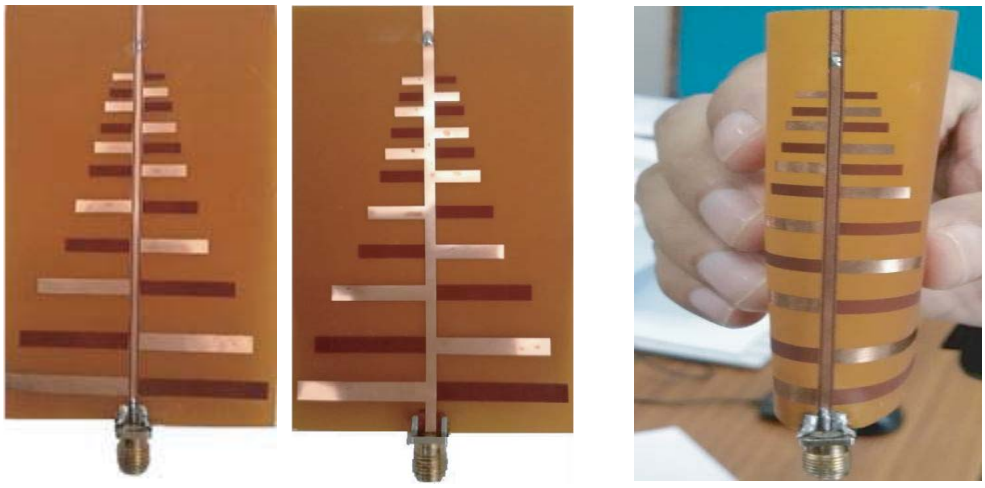

(a) (b) (c)

Figure 2. Fabricated LPDA antenna on the Kapton substrate: (a) Top view (CPW side) and (b) back view (strip side), (c) demonstration of the high LPDA flexibility.

connector, as shown in Fig. 1(c) and Fig. 2. The central conductor is connected to the parallel strip feedline on the back side of the substrate through a conductive *via*, as shown in Fig. 1(d). Here we follow feeding strategy of [23] in which the via along with the stripline and the open-ended CPW ground planes form a balun structure. In this way, the two sides of the paired transmission line setup have opposite currents (with a 180° phase difference), thus exciting the required mode to feed the dipoles [9]. Finally, the length (L_T) between the last element and the via is optimized to achieve required matching and is given by 6.8 mm.

3. MEASUREMENT RESULTS

3.1. Reflection Coefficient

The two measurement setups, i.e., the reflection coefficient (S_{11}) measurement with the Vector Network Analyzer and the pattern determination, are shown in Fig. 3. For the two types of measurements, the LPDA antenna is subjected to different bending conditions. As shown in Fig. 4, the bending position

(a) (b)

Figure 3. Measurement set up for (a) S-parameters using VNA, (b) radiation patterns in an anechoic chamber.

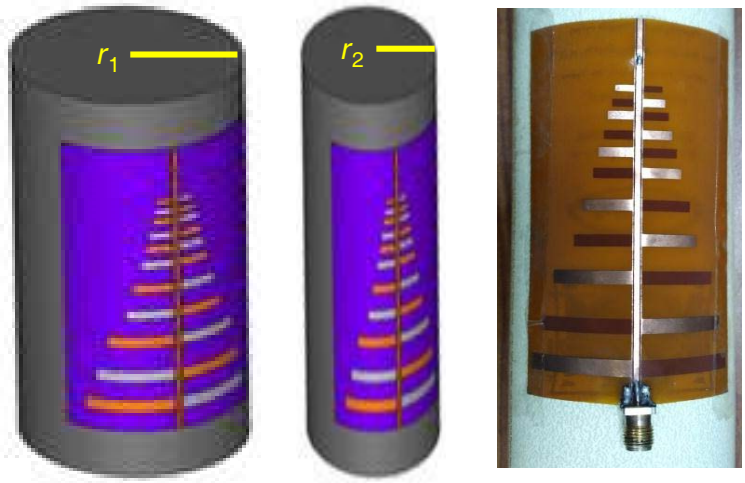

(a) (b) (c)

Figure 4. LPDA in bending position with different curvatures r, (a) HFSS model of an LPDA with a larger bending radius r_1, (b) HFSS model of an LPDA with a smaller bending radius r_2, (c) photograph of the LPDA in the convex bending position with a curvature of $r = 30$ mm.

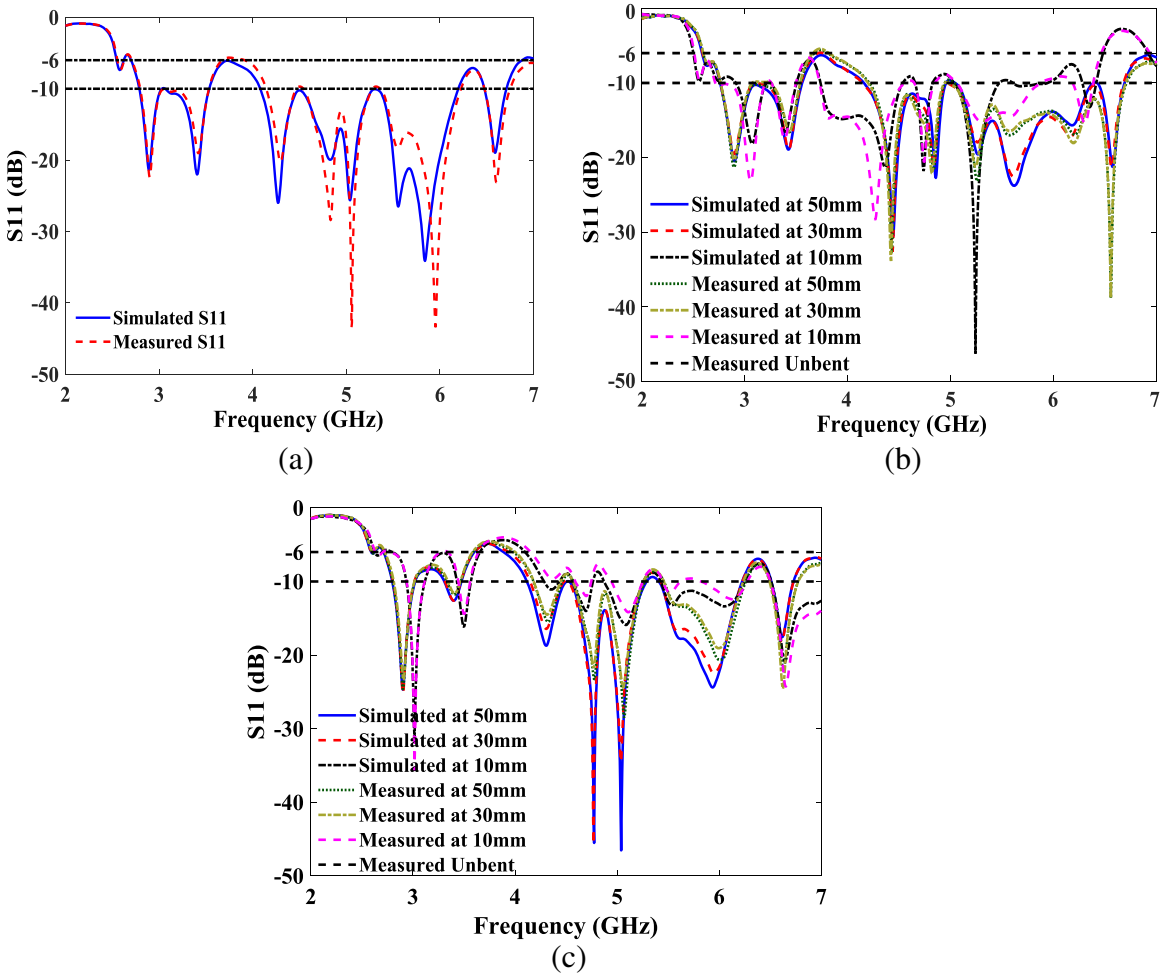

Figure 5. (a) Measured and simulated S_{11} for the LPDA in conventional (non-bending condition), (b) measured and simulated S_{11} for convex bending, (c) measured and simulated S_{11} for concave bending.

is characterized by the curvature of the folded antenna: smaller radius of curvature indicates more bending. The reflection coefficients are measured for three radii of curvature in the convex (when CPW side is inside the curve) and concave bending positions. For each configuration, simulations are performed by the HFSS simulation tool. The simulated and measured reflection coefficients (S_{11}) for the unbent and all bending configurations are provided in Figs. 5(a)–(c). In all the cases, the simulated and measured results are in good agreements. For the flat antenna, the less stringent criterion of 6 dB return loss is satisfied for the entire range of 2.7–6.8 GHz, which is acceptable for many short-range applications [34, 35]. It can also be concluded from Fig. 5(a) that the LPDA can also be employed for the applications which require more stringent 10 dB criterion return loss in the ranges 2.75–3.53 GHz and 4–6.2 GHz. For the bending configurations with the larger radii of curvature of 50 mm and 30 mm, the return loss is similar to the flat antenna case, as depicted in Figs. 5(b) and (c). For the extreme bending curvature of 10 mm, however, a slight degrading performance around 4 GHz can be noted.

3.2. Radiation Patterns

As depicted in Fig. 3(a), the radiation patterns of the proposed LPDA antenna are measured in an anechoic chamber using a broadband horn as a reference antenna. The E and H patterns for the flat (unbent) LPDA and the three convex-curved configurations are shown in Figs. 6(a) and (b). To show the broadband operation, all the patterns are measured at three selected frequencies across the

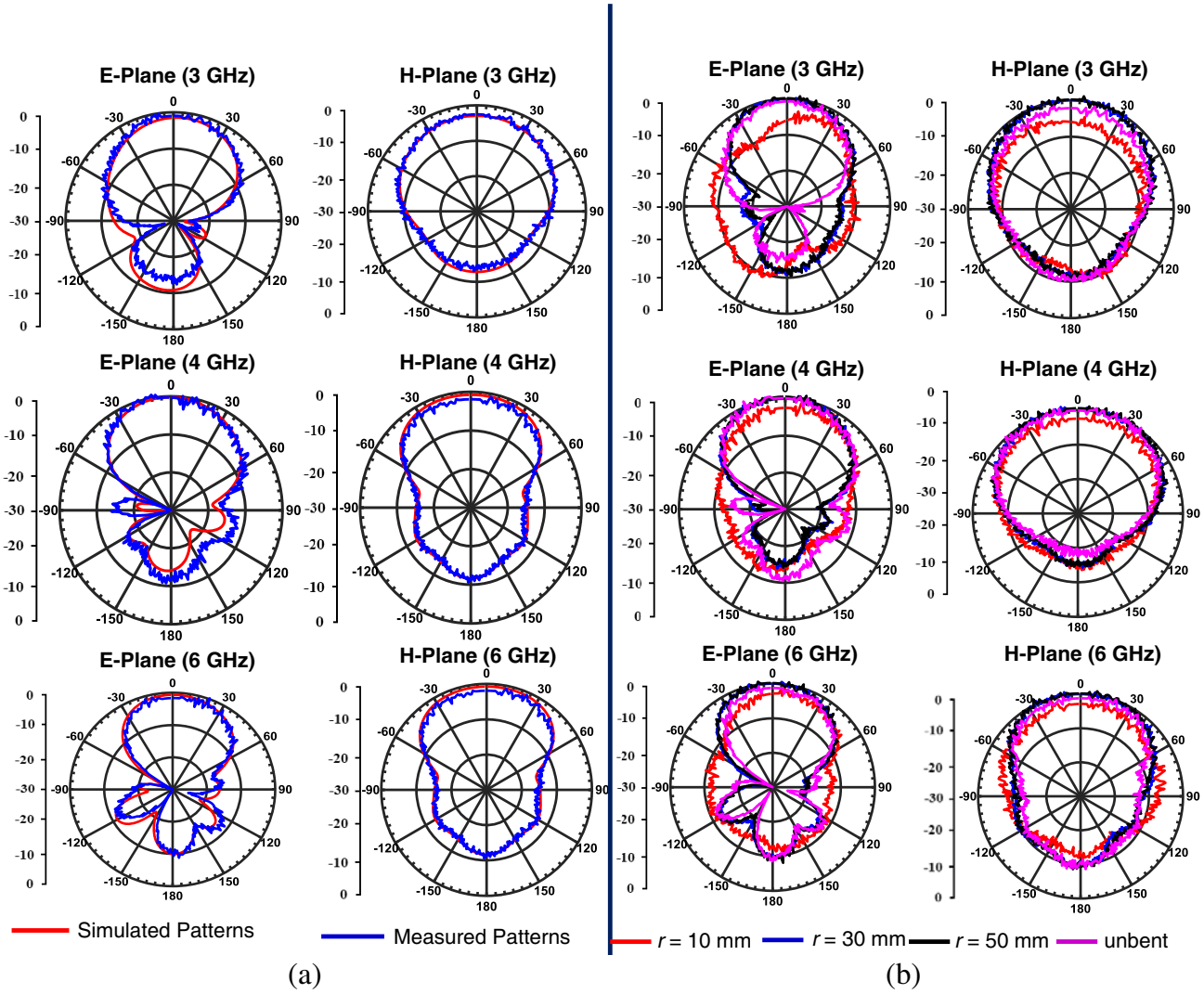

Figure 6. Comparison of the E and H plane radiation patterns at different frequencies for the unbend and bend configurations. (a) Non-bending configuration, (b) convex bending configurations.

spectrum. Considering Fig. 6(a), there is a good agreement between simulation and measured patterns. The end-fire radiation patterns with side lobe levels (SLLs) well below -15 dB are achieved, and the cross-Polarization component is below -20 dB.

With convex-curved configuration of radii 50 mm and 30 mm, shown in the Fig. 6(b), a increase of 0.2 to 0.4 dB in the directivity is noted. This slight increase in the directivity is probably due to the shape deformation of the dipoles which have attained a V-shaped geometry. Note that the radiation patterns for the concave-curved configuration are not shown here because of their similarity to the convex-curved LPDA patterns. Looking at Fig. 6(b), it can be observed that LPDA's H-plane patterns (and hence the gain) are much affected when it is subjected to a bending curvature 10 mm radius. The situation is well anticipated, because in this sharply curved position the edges of the substrate almost touch together, forming a cylindrical structure. However, the antenna still transmits in the end-fire direction at 3 GHz (where the pattern has the largest squint), but with 5 dB less power than the flat antenna.

Finally, consider the frequency versus gain plot along the main beam direction ($\theta = \phi = 0°$), given in Fig. 7. The gain peaks at 5.7 GHz with the value of 6 dBi. In the range 4.9–5.2 GHz, a dip in the gain is due to a small beam squint of not more than $\pm 5°$ (not shown in the radiation patterns). The

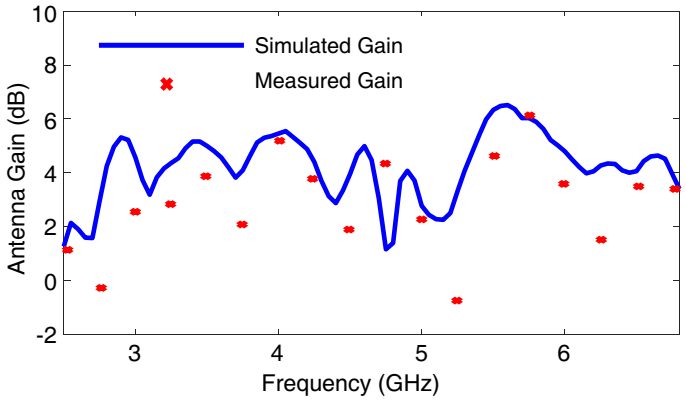

Figure 7. Measured and simulated gain for LPDA without bending.

antenna gain can be increased by choosing the optimum spacing factor $\sigma = 0.15$ in the 7 dB Carrel's design curve [31], but this would increase the device size and affect the compactness feature of the LPDA. Nevertheless, the average gain of the antenna is 4.5 dBi which is a practical compromise, given the additional high bending feature.

4. CONCLUSION

This paper presents a fully characterized flexible LPDA antenna on a Kapton substrate for 3–6 GHz frequency band with a maximum gain of 6 dBi and an average gain of 4.5 dBi across the operating spectrum. The antenna is light weight, economical and only occupies a volume of $90 \times 52 \times 0.035\,\text{mm}^3$. A comprehensive bending analysis is performed which involves folding the antenna about three radii of curvature in the convex and concave configurations. The antenna is matched across the spectrum with minimal gain variation and a return loss better than 6 dB, using a paired CPW-parallel strip combination connected through a conductive via. The end-fire radiation pattern with low side lobe levels is observed in all the bent and unbent configurations. The compact, light weight and flexible design of the antenna makes it a potential candidate for novel communication applications.

REFERENCES

1. Abutarboush, H. F., M. F. Farooqui, and A. Shamim, "Inkjet-printed wideband antenna on resin-coated paper substrate for curved wireless devices," *IEEE Antennas and Wireless Propagation Letters*, Vol. 15, 20–23, 2015.
2. Ahmed, S., F. A. Tahir, A. Shamim, and H. M. Cheema, "A compact Kapton-based inkjet-printed multiband antenna for exible wireless devices," *IEEE Antennas and Wireless Propagation Letters*, Vol. 14, 1802–1805, 2015.
3. Li, W. T., Y. Q. Hei, P. M. Grubb, X.-W. Shi, and R. T. Chen, "Inkjet printing of wideband stacked microstrip patch array antenna on ultrathin flexible substrates," *IEEE Transactions on Components, Packaging and Manufacturing Technology*, Vol. 8, No. 9, 1695–1701, 2018.
4. Tehrani, B. K., B. S. Cook, and M. M. Tentzeris, "Inkjet printing of multilayer millimeter-wave Yagi-Uda antennas on exible substrates," *IEEE Antennas and Wireless Propagation Letters*, Vol. 15, 143–146, 2015.
5. Tang, M.-C., T. Shi, and R. W. Ziolkowski, "Flexible efficient quasi-yagi printed uniplanar antenna," *IEEE Transactions on Antennas and Propagation*, Vol. 63, No. 12, 5343–5350, 2015.
6. Casula, G. A., P. Maxia, G. Mazzarella, and G. Montisci, "Design of a printed log-periodic dipole array for ultra-wideband applications," *Progress In Electromagnetics Research C*, Vol. 38, 15–26, 2013.

7. Hamza, S. M., F. A. Tahir, and H. M. Cheema, "A high-gain inkjet-printed UWB LPDA antenna on paper substrate," *International Journal of Microwave and Wireless Technologies*, Vol. 9, No. 4, 931–937, 2017.
8. Bozdag, G. and A. Kustepeli, "Subsectional tapered fed printed LPDA antenna with a feeding point patch," *IEEE Antennas and Wireless Propagation Letters*, Vol. 15, 437–440, 2015.
9. Casula, G. A., G. Montisci, P. Maxia, G. Valente, A. Fanti, and G. Mazzarella, "A low-cost dual-band CPW-fed printed LPDA for wireless communications," *IEEE Antennas and Wireless Propagation Letters*, Vol. 15, 1333–1336, 2015.
10. Presse, A., J.-M. Floch, and A.-C. Tarot, "Flexible VHF/UHF Vivaldi antenna for broadband applications," *Progress In Electromagnetics Research Letters*, Vol. 52, 37–43, 2015.
11. Lin, C.-P., C.-H. Chang, Y.-T. Cheng, and C. F. Jou, "Development of a flexible SU-8/PDMS-based antenna," *IEEE Antennas and Wireless Propagation Letters*, Vol. 10, 1108–1111, 2011.
12. Rumsey, V. H., *Frequency Independent Antennas*, Academic Press, 2014.
13. Stutzman, W. L. and G. A. Thiele, *Antenna Theory and Design*, John Wiley & Sons, 2012.
14. Jacobson, H. P., C. E. Smith, and R. R. Riggs, "High-power steerable short-wave antennas," *IEEE Transactions on Broadcasting*, Vol. 34, No. 2, 186–192, 1988.
15. Chu, Q.-X., X.-R. Li, and M. Ye, "High-gain printed log-periodic dipole array antenna with parasitic cell for 5G communication," *IEEE Transactions on Antennas and Propagation*, Vol. 65, No. 12, 6338–6344, 2017.
16. Zhang, J., P. V. Orlik, Z. Sahinoglu, A. F. Molisch, and P. Kinney, "UWB systems for wireless sensor networks," *Proceedings of the IEEE*, Vol. 97, No. 2, 313–331, 2009.
17. Gragnani, G. L., D. D. Caviglia, and C. Montecucco, "A log-periodic antenna for long range communication within a wireless sensor network system for sea water quality monitoring," *2018 Advances in Wireless and Optical Communications (RTUWO)*, 161–166, 2018.
18. Martha, G. J., E. M. Cesar, P. L. Gustavo, and S. F. Carlos, "Design and implementation of wireless sensor node in 900 MHz and 2.4 GHz bands," *2016 IEEE Colombian Conference on Communications and Computing (COLCOM)*, 1–5, 2016.
19. Kameoka, S., S. Isoda, A. Hashimoto, R. Ito, S. Miyamoto, G. Wada, N. Watanabe, T. Yamakami, K. Suzuki, and T. Kameoka, "A wireless sensor network for growth environment measurement and multi-band optical sensing to diagnose tree vigor," *Sensors*, Vol. 17, No. 5, 966, 2017.
20. Waterhouse, R., *Microstrip Patch Antennas: A Designers Guide*, Springer Science & Business Media, 2013.
21. Abutarboush, H. F. and A. Shamim, "Based inkjet-printed tri-band U-slot monopole antenna for wireless applications," *IEEE Antennas and Wireless Propagation Letters*, Vol. 11, 1234–1237, 2012.
22. Abutarboush, H. F., H. Nasif, R. Nilavalan, and S. W. Cheung, "Multiband and wideband monopole antenna for GSM900 and other wireless applications," *IEEE Antennas and Wireless Propagation Letters*, Vol. 11, 539–542, 2012.
23. Casula, G. A., P. Maxia, G. Montisci, G. Mazzarella, and F. Gaudiomonte, "A printed LPDA fed by a coplanar waveguide for broadband applications," *IEEE Antennas and Wireless Propagation Letters*, Vol. 12, 1232–1235, 2013.
24. Anim, K. and Y.-B. Jung, "Shortened log-periodic dipole antenna using printed dual-band dipole elements," *IEEE Transactions on Antennas and Propagation*, Vol. 66, No. 12, 6762–6771, 2018.
25. Hsu, H.-T. and T.-J. Huang, "A koch-shaped log-periodic dipole array (LPDA) antenna for universal ultra-high-frequency (UHF) radio frequency identification (RFID) handheld reader," *IEEE Transactions on Antennas and Propagation*, Vol. 61, No. 9, 4852–4856, 2013.
26. Bishop, N. A., J. Miller, D. Zeppettella, W. Baron, J. Tuss, and M. Ali, "A broadband high-gain bi-layer LPDA for UHF conformal load-bearing antenna structures (CLASs) applications," *IEEE Transactions on Antennas and Propagation*, Vol. 63, No. 5, 2359–2364, 2015.
27. Chang, L., S. He, J. Q. Zhang, and D. Li, "A compact dielectric-loaded log-periodic dipole array (LPDA) antenna," *IEEE Antennas and Wireless Propagation Letters*, Vol. 16, 2759–2762, 2017.

28. Anagnostou, D. E., J. Papapolymerou, M. M. Tentzeris, and C. G. Christodoulou, "A printed log-periodic koch-dipole array (LPKDA)," *IEEE Antennas and Wireless Propagation Letters*, Vol. 7, 456–460, 2008.
29. Gheethan, A. A. and D. E. Anagnostou, "Reduced size planar log-periodic dipole arrays (LPDAS) using rectangular meander line elements," *2008 IEEE Antennas and Propagation Society International Symposium*, 1–4, IEEE, 2008.
30. Yagyu, H., S. Ifuku, and M. Nogi, "Acetylation of optically transparent cellulose nanopaper for high thermal and moisture resistance in a flexible device substrate," *Flexible and Printed Electronics*, Vol. 2, No. 1, 014003, 2017.
31. Carrel, R., "The design of log-periodic dipole antennas," *1958 IRE International Convention Record*, Vol. 9, 61–75, IEEE, 1966.
32. Balanis, C. A., *Antenna Theory: Analysis and Design*, John Wiley & Sons, 2016.
33. Wadell, B. C., *Transmission Line Design Handbook*, Artech House, 1991.
34. Waterhouse, R., *Printed Antennas for Wireless Communications*, Vol. 19, John Wiley & Sons, 2008.
35. Chang, T.-N. and Y.-L. Chan, "Antenna with two folded strips coupled to a T-shaped monopole," *Progress In Electromagnetics Research M*, Vol. 60, 197–207, 2017.